Asymmetric square waves in mutually coupled semiconductor lasers with orthogonal optical injection

David W. Sukow,[1],* Athanasios Gavrielides,[2] Thomas Erneux,[3] Benjamin Mooneyham,[1] Karen Lee,[1] Jake McKay,[1] and Josiah Davis[1]

[1]*Department of Physics and Engineering, Washington and Lee University, 204 W. Washington St., Lexington, Virginia 24450, USA*
[2]*Air Force Research Laboratory, AFRL/EOARD, 86 Blenheim Crescent, Ruislip Middlesex HA4 7HB, United Kingdom*
[3]*Optique Nonlinéaire Théorique, Université Libre de Bruxelles, Campus Plaine, CP 231, 1050 Bruxelles, Belgium*

Two edge-emitting lasers mutually coupled through orthogonal optical injection exhibit square-wave oscillations in their polarization modes. The TE and TM modes within each individual laser are always in antiphase, but the TE mode of one laser leads the TM of the other by the one-way time of flight between lasers. The duty cycle of the square waves is tunable with pump current and coupling strength, while the total period remains close to the roundtrip time. Numerical simulations give similar results and reveal the role of noise in stabilizing the oscillations.

Delay-differential systems are of great importance in most fields of basic and applied sciences. They appear readily in control systems in which feedback is reinjected after a time delay, with examples that abound in biology, chemistry, mechanical systems, traffic flow, and others [1]. Nonlinear optical systems in particular, with feedback that is nonlocal in space and time, are subjects of continuous interest in several applications, including phase distortion suppression and stabilization, optical beam shaping, pattern formation, and all-optical image processing.

A fundamental property of many nonlinear dynamical systems is bistability as typified by double-well systems and those displaying hysteresis. Two-state solutions form the basis of all binary logic applications, and examples are plentiful in electronics, beginning with the most common multivibrator circuits used for logic, clocks, and gates. Optical digital logic is an area of rapidly increasing importance, with optical data storage and telecommunications as primary applications, as well as resurgent interest in optical computing. Therefore, two-state laser systems are of critical importance. There are a variety of useful applications stemming from the all-optical production of high-frequency optical pulses [2].

Recent work has emphasized semiconductor laser systems [edge-emittings lasers spectroscopy (EELs) and vertical-cavity surface-emitting lasers (VCSELs)] with polarization-rotated feedback [3–7] as a source of optical square pulses generated through polarization self-modulation [8–12]. These solutions are of fundamental interest in part because their dynamic properties can be examined in more detail than for conventional (nonrotated) optical feedback and because they relate to optoelectronic systems [13,14]. Pulse trains generated in all such single-laser systems are symmetric square waves with duty cycles of 0.5.

This paper describes optical generation of pulse trains in a system of two mutually coupled semiconductor lasers. Experimentally, we observe solutions of square pulse trains with duty cycles that are *tunable* as functions of the coupling strength and pump current. Self-consistent timing relationships between polarization modes are observed, and similar solutions are obtained through numerical simulations.

For an overview, the dynamical system consists of two EELs, mutually coupled through optical injection, where the linear polarization state of each injected beam is rotated orthogonal to its initial orientation. The EELs exhibit a dominant linear polarization mode and are mounted such that their TE modes are oriented horizontally. Rotators in the injection path accomplish a net 90° rotation of both beams, so the TE mode of each laser is injected into the TM mode of the other. This is the only coupling between the lasers; TM outputs of the lasers are extinguished in the cavity.

The apparatus is shown schematically in Fig. 1. The two diode lasers (LD1 and LD2) are model SDL-5401 index guided Fabry-Perot MQW devices stabilized in temperature to ±0.01 °C. The lasers have nominal wavelengths of λ =818 nm and solitary current thresholds of 18.5 mA. Their beams encounter identical collimating lenses (CL) with numerical apertures of 0.47. The injection path is shown as the U-shaped heavy line in the diagram and the two beams counterpropagate along it, encountering the same sequence of optical components. Each beam is sampled by a 5% reflective beamsampler (BS) and then is directed through a Faraday rotator (ROT) with its input polarizer removed. Upon passing through the rotator, each beam rotates 45° from the hori-
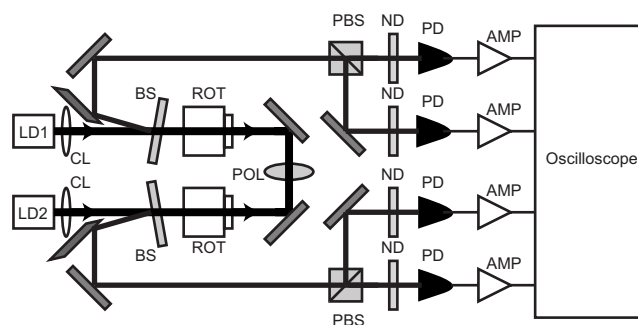

FIG. 1. Schematic diagram of experimental apparatus. Definitions of abbreviations are in the text.
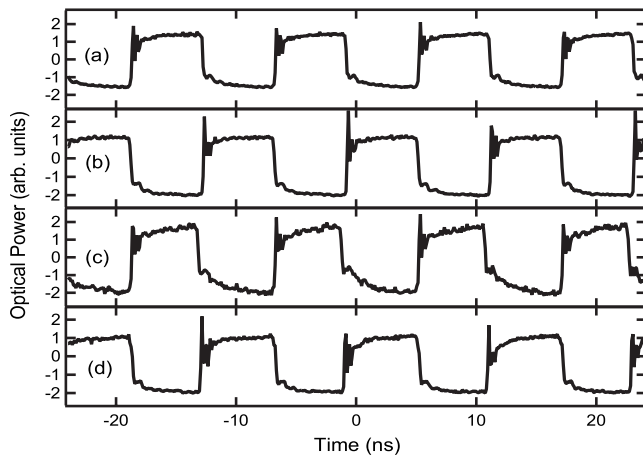
*sukowd@wlu.edu

FIG. 2. Time series of experimentally observed square waves showing TM and TE modes of [(a) and (b)] laser 1 and [(c) and (d)] laser 2.

FIG. 3. Time series of experimentally observed asymmetric square waves, showing TM and TE modes of [(a) and (b)] laser 1 and [(c) and (d)] laser 2.

zontal and emerges from the output polarizer of the rotator. They then reflect from two steering mirrors with a rotatable linear polarizer (POL) between them, which is used for injection strength control. All unlabeled components in Fig. 1 are high-reflectivity mirrors. Each beam then enters the second Faraday rotator through its 45° output polarizer, passes through, and rotates to a vertical linear polarization state. In this form, it is injected into the other laser, coupled to its TM mode which is normally suppressed. Note that any TM emission from either laser does not take part in the mutual coupling since any vertically oriented light that enters the Faraday rotator will strike the output polarizer orthogonal to its transmission axis and will therefore be extinguished. This applies to TM light emitted via lasing action or reflected from the laser's front facet.

The dynamics of this system are detected using the beams deflected from the BSs placed in each line immediately after they emerge from the collimating lenses. The beams strike the samplers at near-normal incidence to minimize polarization-dependent effects in the Fresnel reflections. We separate each of the two sampled beams into TE and TM components using a polarizing beamsplitter (PBS) cube for polarization-resolved detection. We attenuate the beams using neutral density (ND) filters before they strike the photodetectors (PDs). The ac signals from these 8.75 GHz detectors (Hamamatsu C4258–01) are amplified by 23 dB using wideband (10 kHz–12 GHz) amplifiers and are captured and analyzed by a digital storage oscilloscope (LeCroy 8600, 5 GHz analog bandwidth, 10 GS/s sampling rate).

Using this experimental setup, we observe a variety of dynamical effects in the time domain, including square waveforms as shown in Fig. 2. In this case, the pump currents I_1 and I_2 both are 38.88 mA. Laser LD1 is stabilized at a temperature of 20.02 °C and LD2 at 19.01 °C. The delay $\tau = 5.57$ ns, and the coupling strength is quantified as a one-way fractional transmission of 48.7% through the cavity. Figures 2(a) and 2(b) show the TM and TE modes of LD1, respectively, and Figs. 2(c) and 2(d) show the same for LD2. These operational conditions yield square waves with a duty cycle of 0.5 in all polarization modes, and several features
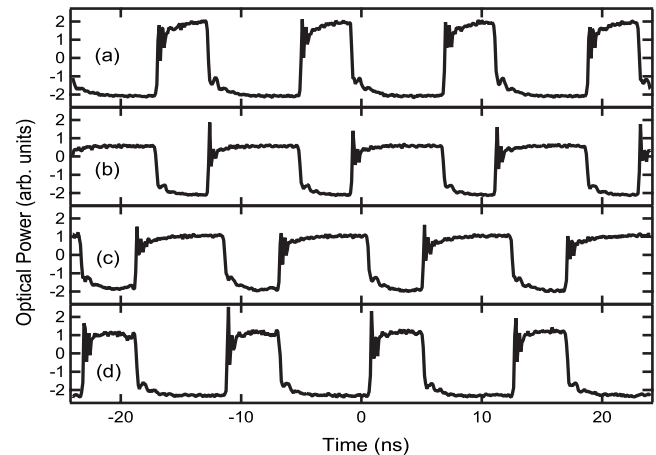
are evident. First, for each individual laser, the TE and TM modes are in antiphase. This demonstrates how the lasers switch between TE and TM operation, thus generating polarization-modulated square waves. A second observation is that the TE modes for both lasers are on simultaneously, followed by an equal duration when both TM modes are active. Third, the period of the square waveform is 11.9 ns, which is close to but slightly greater than the cavity roundtrip time, 2τ. Since the period is governed by τ, it is adjustable as has been verified using several cavity lengths. Finally, on a faster time scale, high-frequency relaxation oscillations appear at the onset of each switching event.

This can be interpreted physically as follows. If LD1 and LD2 turn on simultaneously from off states, with no optical power present in the cavity, each laser acts at first as a solitary laser, emitting in its natural TE mode which propagates into the injection path. This represents the stage when the TE mode is on in both lasers. After a duration τ, the beams from each laser will have propagated through the entire injection path, having been rotated 90° in polarization in the process, and reach the other laser. Upon injection, the TM mode lases dominantly, shutting off the TE mode. The TM modes operate as long as the injection drives them, which will also be equal to τ, since the TE source has been shut off after that time. This is the stage when both TM modes are on. After this second interval of τ has elapsed, there is no longer any injection due to TE emission and TM emission ends. Thus the lasers return to a solitary state with no power in the cavity, and the process repeats. A very similar process takes place in single-laser systems with orthogonal optical feedback, which can also produce square waves [8–12].

This scenario is intuitively logical but does not fully explain all observations in this system. For example, Fig. 3 demonstrates another self-consistent solution: square waves with duty cycles other than 0.5. The ordering of the graphs is the same as before: Figs. 3(a) and 3(b) show the TM and TE modes of LD1, respectively, and Figs. 3(c) and 3(d) show the same for LD2. Many of the key elements are the same as before. The period of the waves is still 11.9 ns. In addition, the TE and TM modes remain in antiphase within each indi-
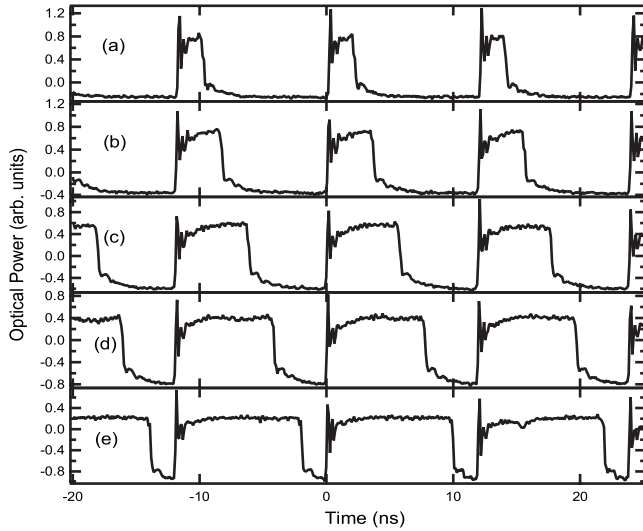
FIG. 4. Experimental square waves with variable duty cycle as a function of pump current. Only the TE mode of LD2 is illustrated for clarity.
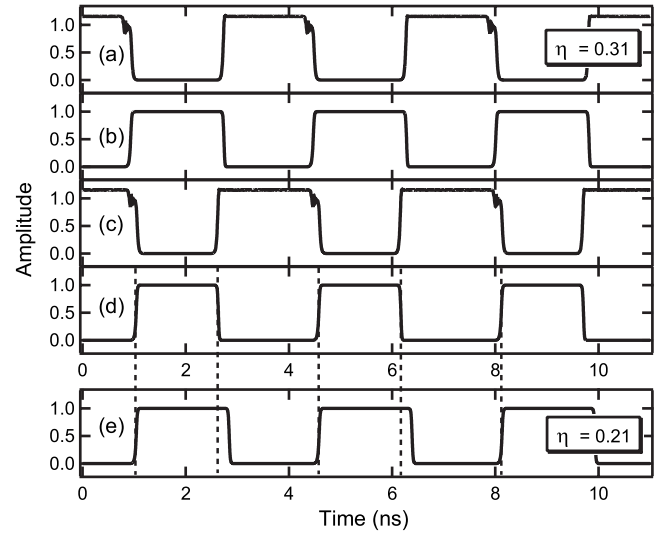

FIG. 5. Numerical solutions showing (A_n^v, A_n^h) for [(a) and (b)] laser 1 and [(c) and (d)] laser 2 with $\eta=0.31$; A_2^h with $\eta=0.21$ changes duty cycle (e).

vidual laser. However, the TE and TM on phases are no longer equal in duration. For example, the TM wave in Fig. 3(a) is on for only 4.3 ns and thus has a duty cycle of 0.36, whereas the accompanying TE mode in Fig. 3(b) lasts 7.6 ns (duty cycle 0.64). Furthermore, the situation is reversed for Figs. 3(c) and 3(d), so unlike the nearly identical TM square waves in Figs. 2(a) and 2(c), Figs. 3(a) and 3(c) are now dissimilar. For these data, the coupling is reduced to 46.6 %, but other experimental conditions remain the same.

The self-consistency of this asymmetric solution requires that the TE and TM modes of each individual laser be in antiphase, and any TE pulse in one laser must induce a similar TM pulse in the other laser a time τ later. The waves in Fig. 3 display these characteristics. The two pairs of signals [Figs. 3(a) and 3(b); Figs. 3(c) and 3(d)] are in antiphase. In addition, the TE wave in Fig. 3(b) is reproduced with a delay of τ in the TM wave in Fig. 3(c), and the same applies to waves in Figs. 3(d) and 3(a).

The duty cycle can be changed continuously via experimentally accessible controls: coupling strength and pump currents. If the coupling is too weak or the pump currents too dissimilar, the system cannot maintain square-wave operation. To illustrate this effect, Fig. 4 shows five time series at different values of I_2 while I_1 is fixed at 34.5 mA. Rather than showing all four polarization modes as in the two previous figures, Fig. 4 presents only the TE mode of LD2 for visual clarity. The coupling strength is 62.8%. The currents for Figs. 4(a)–4(e) have values of 33.5, 33.8, 34.1, 34.5, and 34.8 mA, respectively. The lowest and highest duty cycles shown are 0.18 and 0.84, respectively. All of these waveforms have stable duty cycles over several minutes in the absence of external perturbations. Outside of this range of currents the duty cycle approaches 0 or 1.

We use a set of six rate equations to model the system of two EELs crosscoupled by TE to TM injection. The equations for each individual laser are similar to those used by Heil *et al.* [15] but are expressed in dimensionless form [16] for the complex TE and TM fields E^h and E^v, respectively,

and the carrier density Z. The two different lasers are denoted by subscripts 1 and 2. The coupling of each laser's TE mode into the other's TM mode is described with time-delayed terms in the equation for E_1^v and E_2^v. The coupled laser equations then are

$$\frac{dE_n^h}{dt} = (1 + i\alpha)Z_n E_n^h + \xi_n^h, \quad (1)$$

$$\frac{dE_n^v}{dt} = (1 + i\alpha)k(Z_n - \beta)E_n^v + \eta E_{3-n}^h(t - \tau) + \xi_n^v, \quad (2)$$

$$T\frac{dZ_n}{dt} = P_n - Z_n - (1 + 2Z_n)(|E_n^h|^2 + |E_n^v|^2), \quad (3)$$

where $n=1$ or 2. The rapidly varying random forcing terms $\xi_n^h(t)$ and $\xi_n^v(t)$ have zero mean and an autocorrelation function given by $\langle \xi_n^k(t)\xi_m^l(t')\rangle = 2D\delta_{nm}\delta^{kl}\delta(t-t')$, where $k, l=h$ or v and $n, m=1$ or 2. The dimensionless time $t=t'/\tau_h$ is normalized by the cavity lifetime τ_h of the horizontal mode. The gain parameter $k=g_h/g_v$ is the ratio of the two gains, η is the normalized feedback strength, and $\beta=\frac{1}{2}(\frac{g_h\tau_h}{g_v\tau_v}-1)>0$ represents the differential losses where τ_h and τ_v are the cavity lifetimes of the horizontal and vertical modes, respectively. The parameter β depends on both gains and losses but is positive so that E^h is the fundamental lasing mode of both lasers in the absence of feedback. The parameter α is the linewidth enhancement factor and $T=\tau_s/\tau_h$ is the ratio of the carrier to cavity lifetimes. We assume that both lasers admit the same values of the fixed parameters α and T but the pump parameters P_1 and P_2 can be controlled independently.

Figure 5 shows numerical time series of the amplitude of the fields $A_1^{v,h}=|E_1^{v,h}|$ and $A_2^{v,h}=|E_2^{v,h}|$. Parameters used in these simulations are $T=100$, $\tau=3000$, $\tau_h=2.5$ ps, $\alpha=2$, $\beta=0.03$, $k=1$, $P_1=P_2=1.0$, and noise correlation 3.0×10^{-9}. For initial conditions we also use noise of the same correla-

tion over the interval $-\tau < t < 0$. Graphs (a)–(d) are displayed in the same order as in Fig. 3 and have $\eta = 0.31$. The wave forms are rectangular with asymmetry, as found experimentally, and the period is equal to twice the time separation between the lasers. Graph (e) shows A_2^h for $\eta = 0.21$ and reproduces the effect of changing the asymmetry of the wave. This is easily seen by comparing graphs (d) and (e), guided by the dashed vertical lines. In other simulations, increasing P_n increases the on duration of E_n^h; the specific effect of varying η depends on other system parameters.

Within each laser the TE and TM waves oscillate in antiphase ($A_n^h \neq 0$, $A_n^v = 0$ and then $A_n^h = 0$, $A_n^v \neq 0$), but between lasers a timing relation exists for the TE and the injected TM modes (A_n^v versus A_{3-n}^h) as observed experimentally. This can be understood by eliminating adiabatically E_n^v from Eq. (2) and using the fact that $Z_n / \sqrt{\tau} \ll 1$ as in [17]. We find

$$E_n^v \approx \frac{\eta}{(1 + i\alpha)k\beta} E_{3-n}^h (t - \tau), \tag{4}$$

where $n = 1, 2$.

The square waves switch between two pure mode steady-state solutions of Eqs. (1)–(3), namely, (1) $A_1^h \neq 0$, $A_2^v \neq 0$, $A_1^v = A_2^h = 0$ and (2) $A_1^v \neq 0$, $A_2^h \neq 0$, $A_1^h = A_2^v = 0$. This switching is delayed between lasers by τ due to the lag inherent in the delayed driving terms. The square waveforms appear not to be asymptotic states but are long transients that decay to either of these steady states by slowly reducing the on duration of one of them. This essentially is the physical mechanism responsible for the asymmetry in the on durations. However, we have found that an appropriate amount of noise

contributes to the stabilization of these square-wave transients as observed in other laser systems [18]. In our simulations, the duration of the square waves may persist (in real time) from a few microseconds to milliseconds depending on the initial conditions and the level of noise. Metastable responses where fast transition layers between plateaus are slowly moving are known for delay differential equations and have been studied in [19]. The stabilizing effects of noise have also been analyzed in [20].

In summary, we have experimentally observed polarization-modulated rectangular pulse trains with variable duty cycle in a system of two EELs, mutually coupled through orthogonal optical injection of each laser's TE mode into the other's TM mode. The TE and TM waves within each individual laser are in antiphase, and the TE mode of one laser leads the TM mode of the other by a time delay τ equal to the one-way photon time of flight in the external cavity. Numerical simulations reproduce the polarization modulated square waves and highlight the role of noise in stabilizing the waves. Both experiments and numerical simulations indicate variable duty cycles as a function of the coupling strength and pump current and the details will be documented elsewhere.

[1] T. Erneux, *Applied Delay Differential Equations* (Springer, New York, 2009).

[2] J.-L. Cheng and T.-S. Yen, Opt. Commun. **271**, 503 (2007).

[3] K. Otsuka and J. L. Chern, Opt. Lett. **16**, 1759 (1991).

[4] T. C. Yen, J. W. Chang, J. M. Lin, and R. J. Chen, Opt. Commun. **150**, 158 (1998).

[5] J. Houlihan, G. Huyet, and J. G. McInerney, Opt. Commun. **199**, 175 (2001).

[6] F. Rogister, A. Locquet, D. Pieroux, M. Sciamanna, O. Deparis, P. Megret, and M. Blondel, Opt. Lett. **26**, 1486 (2001).

[7] N. Shibasaki, A. Uchida, S. Yoshimori, and P. Davis, IEEE J. Quantum Electron. **42**, 342 (2006).

[8] W. H. Loh, Y. Ozeki, and C. L. Tang, Appl. Phys. Lett. **56**, 2613 (1990).

[9] F. Robert, P. Besnard, M. L. Charles, and G. M. Stephan, IEEE J. Quantum Electron. **33**, 2231 (1997).

[10] H. Li, A. Hohl, A. Gavrielides, H. Hou, and K. Choquette, Appl. Phys. Lett. **72**, 2355 (1998).

[11] A. Gavrielides, T. Erneux, D. W. Sukow, G. Burner, T. McLachlan, J. Miller, and J. Amonette, Opt. Lett. **31**, 2006 (2006).

[12] J. Mulet, M. Giudici, J. Javaloyes, and S. Balle, Phys. Rev. A **76**, 043801 (2007).

[13] P. Saboureau, J.-P. Foing, and P. Schanne, IEEE J. Quantum Electron. **33**, 1582 (1997).

[14] J. M. Saucedo Solorio, D. W. Sukow, D. R. Hicks, and A. Gavrielides, Opt. Commun. **214**, 327 (2002).

[15] T. Heil, A. Uchida, P. Davis, and T. Aida, Phys. Rev. A **68**, 033811 (2003).

[16] A. Gavrielides, T. Erneux, D. W. Sukow, G. Burner, T. McLachlan, J. Miller, and J. Amonette, Proc. SPIE **6115**, 61150M (2006).

[17] D. W. Sukow, A. Gavrielides, T. Erneux, M. J. Baracco, Z. A. Parmenter, and K. L. Blackburn, Phys. Rev. A **72**, 043818 (2005).

[18] Q. L. Williams, J. Garcia-Ojalvo, and R. Roy, Phys. Rev. A **55**, 2376 (1997).

[19] K. Pakdaman, C. P. Malta, C. Grotta-Ragazzo, O. Arino, and J.-F. Vibert, Phys. Rev. E **55**, 3234 (1997); K. Pakdaman, C. Grotta-Ragazzo, and C. P. Malta, *ibid.* **58**, 3623 (1998); C. Grotta-Ragazzo, K. Pakdaman, and C. P. Malta, *ibid.* **60**, 6230 (1999).

[20] R. Kuske, L. F. Cordillo, and P. Greenwood, J. Theor. Biol. **245**, 459 (2007); M. M. Klosek and R. Kuske Multiscale Model. Simul. **3**, 706 (2005).